INTERNATIONAL JOURNAL FOR NUMERICAL METHODS IN FLUIDS, VOL. 6, 351–364 (1986)

APPLICATION OF A PRESSURE GRADIENT METHOD TO AN FEM FLOW ANALYSIS

YOSHIHIRO MOCHIMARU

Department of Mechanical Engineering, Tokyo Institute of Technology, Tokyo 152, Japan

SUMMARY

A pressure gradient method employing pressure gradients as dependent variables is applied to a finite-element-method flow analysis for a two-dimensional incompressible Newtonian fluid flow. In a numerical analysis, a triangular element is adopted, a velocity vector and a pressure gradient vector being assigned as dependent variables at the nodal points. Velocity and pressure gradient are interpolated linearly in space, and a discretizing formulation can be made using a suitably selected weighting function. An example of application is shown for an unsteady-state development of a recirculating circular cavity flow, the numerical results to which are in good agreement with those obtained analytically or by other numerical means.

KEY WORDS Pressure Gradient Method FEM Unsteady Flow Cavity Flow

1. INTRODUCTION

In the numerical simulation of fluid flows, finite element methods have become greatly practicable in the past decade, probably in connection with the advantage of incorporating almost any complex boundaries and/or complex flow fields, and thus various techniques for practical application have been devised,[1,2] whereas application of finite difference techniques, unless interpolation or extrapolation techniques are introduced for locations of boundaries, is originally limited mainly to problems for the spatial regions of which regular (not necessarily uniform) meshes can be generated or for the whole region of which a mapping (usually a conformal mapping) to a region possessing boundaries of geometrically simple shape is possible.[3] Thus the finite element procedures for numerical simulation of flow have penetrated into broad areas of fluid mechanics,[1,2,4,5] which has necessitated various matters to be discussed, such as error estimation,[5,6] selection of the number and location of nodal points for better discretization in space, selection of the kind and degree of interpolation functions and weighting functions, and selection of dependent variables. Of these factors, selection of variables determines the form of a fundamental set of equations to be solved and consequently affects the nature of the other factors. For an isothermal laminar incompressible Newtonian fluid flow, a set of a velocity vector and pressure or a set of a stream function and vorticity (in the case of a two-dimensional/axisymmetric flow) has been widely adopted as primitive dependent variables not only in a finite element procedure but in a finite difference procedure. Alternatively, use of a different set of dependent variables, i.e. a set of a velocity vector and a pressure gradient vector, has been proposed in finite difference techniques;[3,7] such a method is called a pressure gradient method.

So, in the current paper, concrete techniques and procedures for application of a pressure

0271–2091/86/060351–14$07.00

Received 25 October 1985
Revised 16 January 1986

gradient method to an FEM flow analysis are proposed with a special attention to the treatment of boundary conditions. Also given is an example of the analysis applied to an unsteady-state development of a recirculating circular cavity flow.

ANALYSIS

Formulation by finite element techniques using a pressure gradient method

Although a pressure gradient method can be applied both in a two-dimensional flow and in a three-dimensional flow, as in the case of a finite difference method,[7] for simplicity notation is limited to the case of a two-dimensional isothermal laminar incompressible Newtonian fluid flow. Hereafter use is made of dimensionless quantities, that is, all the quantities that will appear have already been made dimensionless with respect to either the reference speed U_0, the reference pressure ρU_0^2, the reference length L, or the reference time L/U_0, where ρ, U_0 and L denote the density of fluid considered, a characteristic speed in a flow field and a characteristic length in a flow field, respectively. Now, let a velocity vector $\mathbf{V}$ and a pressure gradient vector ∇p be regarded as dependent variables. Then the equations to be solved are the equation of motion

$$\frac{\partial}{\partial t}\mathbf{V} + (\mathbf{V}\cdot\nabla)\mathbf{V} = -\nabla p + \frac{1}{Re}\Delta\mathbf{V}, \tag{1}$$

the equation of continuity

$$\nabla\cdot\mathbf{V} = 0 \tag{2}$$

and the compatibility condition

$$\text{curl}\quad(\nabla p) = \mathbf{0}, \tag{3}$$

where Re denotes a Reynolds number and is defined as

$$Re = \rho L U_0/\mu,$$

μ being the viscosity of the fluid, and to simplify the expression, only external body forces having a potential, such as gravity, are taken into account to be included in the pressure. As for division of space, triangular elements fixed in space are used, and nodal points, which are common for $\mathbf{V}$ and ∇p, are assigned to every apex of each triangular element, as shown in Figure 1. Hereafter $\mathbf{V}$ and ∇p are assumed to be vector fields of class C^2 and of class C^1 in space, respectively. Equations (1)–(3) can be integrated over a subspace consisting of triangular elements to give

$$\frac{\mathrm{d}}{\mathrm{d}t}\int M_1\mathbf{V}\,\mathrm{d}S + \int M_1(\mathbf{V}\cdot\nabla)\mathbf{V}\,\mathrm{d}S = -\int M_1\nabla p\,\mathrm{d}S + \frac{1}{Re}\int M_1\Delta\mathbf{V}\,\mathrm{d}S, \tag{4}$$

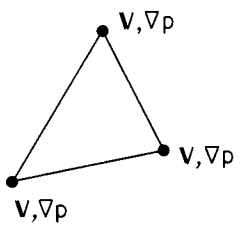

Figure 1. Triangular element. Variables $\mathbf{V}$ and ∇p are assigned to each apex of the element

$$\int M_2 \nabla \cdot \mathbf{V}\, dS = 0, \tag{5}$$

$$\int M_3 \mathrm{curl}(\nabla p) \cdot d\mathbf{S} = 0, \tag{6}$$

where the subspace is a simply connected region keeping inside one and only one apex common to all triangular elements belonging to the subspace; M_1, M_2 and M_3 are weighting functions such that $\nabla M_i (i = 1, 2, 3)$ is piecewise continuous and that $M_i (i = 1, 2, 3)$ is continuous; and $d\mathbf{S}$ is an area vector normal to the surface element. By the Gauss theorem, equations (4) and (5) become

$$\frac{d}{dt}\int M_1 \mathbf{V}\, dS - \int (\nabla M_1 \cdot \mathbf{V})\mathbf{V}\, dS + \oint M_1 (\mathbf{V} \cdot \mathbf{n})\mathbf{V}\, dc$$
$$= -\int M_1 \nabla p\, dS + \frac{1}{Re}\left\{\oint M_1 (\mathbf{n} \cdot \nabla)\mathbf{V}\, dc - \int (\nabla M_1 \cdot \nabla)\mathbf{V}\, dS\right\}, \tag{7}$$

$$\oint M_2 \mathbf{V} \cdot \mathbf{n}\, dc - \int \nabla M_2 \cdot \mathbf{V}\, dS = 0, \tag{8}$$

respectively, where use is made of equation (2). By the Stokes theorem, equation (6) becomes

$$\oint M_3 \nabla p \cdot d\mathbf{c} - \int (\nabla M_3 \times \nabla p) \cdot d\mathbf{S} = 0. \tag{9}$$

In equations (7)–(9), $d\mathbf{c}$ and $\mathbf{n}$ denote a line-element vector along the contour of the domain of integration and an outward unit normal (parallel to the flow plane) at the contour, respectively, and $dc = |d\mathbf{c}|$. All the more, if the M_is are chosen so that they vanish on the contour of integration, then equations (7)–(9) become

$$\frac{d}{dt}\int M_1 \mathbf{V}\, dS - \int (\nabla M_1 \cdot \mathbf{V})\mathbf{V}\, dS = -\int M_1 \nabla p\, dS - \frac{1}{Re}\int (\nabla M_1 \cdot \nabla)\mathbf{V}\, dS, \tag{10}$$

$$\int \nabla M_2 \cdot \mathbf{V}\, dS = 0, \tag{11}$$

$$\int (\nabla M_3 \times \nabla p) \cdot d\mathbf{S} = 0, \tag{12}$$

respectively.

Discretization of equation (10)

Using a forward difference formula with respect to the time derivative, equation (10) can be replaced by

$$\frac{1}{\delta t}\left\{\left(\int M_1 \mathbf{V}\, dS\right)_{t+\delta t} - \left(\int M_1 \mathbf{V}\, dS\right)_t\right\} - \left(\int (\nabla M_1 \cdot \mathbf{V})\mathbf{V}\, dS\right)_t$$
$$= -\left(\int M_1 \nabla p\, dS\right)_{t+\delta t} - \frac{1}{Re}\left(\int (\nabla M_1 \cdot \nabla)\mathbf{V}\, dS\right)_{t+\delta t}, \tag{13}$$

under the assumption that triangular elements are fixed in space. In equation (13) the subscripts t and $t + \delta t$ denote the time when $\mathbf{V}$ or ∇p appearing in each integrand is to be evaluated, and

δt (> 0) is a time increment between two successive time steps. When carrying out the integration in equation (13), $\mathbf{V}$ and ∇p in each triangular element (including its contour) are supposed to be linearly interpolated in space in terms of linear shape functions, i.e. area co-ordinates[8,9] and the values at nodal points as follows:

$$\mathbf{V} = \sum_{k=1}^{3} N_k \mathbf{V}_k, \tag{14}$$

$$\nabla p = \sum_{k=1}^{3} N_k \nabla p_k, \tag{15}$$

where N_k, $\mathbf{V}_k$ and ∇p_k denote an area co-ordinate, the velocity vector at a nodal point, and the pressure gradient at the nodal point, respectively, and the latter two vectors may be functions of time. Thus equation (13) can be completely discretized using values at nodal points.

Discretization of the equation of continuity and the compatibility condition

Using the same interpolation expressions (14) and (15), the discretized forms of the equation of continuity and the compatibility condition can be obtained through the following:

$$\left(\int \nabla M_2 \cdot \mathbf{V} \, \mathrm{d}S \right)_{t+\delta t} = 0, \tag{16}$$

$$\left(\int (\nabla M_3 \times \nabla p) \cdot \mathrm{d}\mathbf{S} \right)_{t+\delta t} = 0. \tag{17}$$

Improvement of the discretized form of equation (16)

If M_2 is a polynomial function of one area co-ordinate that assume a value of unity when the point (x, y) coincides with the common nodal point $\mathbf{x}^0$, as shown in Figure 2, or of that co-ordinate followed by an arbitrary exponent (> 0), then the coefficient of $\mathbf{V}$ at $\mathbf{x}^0$ vanishes identically in the discretized form of equation (16). This discretized form necessarily involves relative truncation errors, if the $\mathbf{V}_k$s are exact, of the order of

$$\frac{h^2 \left\| \left(\dfrac{\partial^2}{\partial x^2}, \dfrac{\partial^2}{\partial x \, \partial y}, \dfrac{\partial^2}{\partial y^2} \right) \mathbf{V} \right\|}{\max\limits_{\mathbf{x}^i, \mathbf{x}^j \in S} |\mathbf{V}(\mathbf{x}^i) - \mathbf{V}(\mathbf{x}^j)|}, \tag{18}$$

where h is the characteristic length of the triangular elements and S is the domain of integration.

Therefore, if without loss of generality it is assumed that $M_2 \sim 1$, instead of the discretized form of equation (16) the following form is recommended to obtain better numerical stability:

$$\left(\int \nabla M_2 \cdot \mathbf{V}^* \, \mathrm{d}S \right)_{t+\delta t} + \varepsilon h \left\{ \left(\sum_k \beta_k \mathbf{V}^k - \mathbf{V}^0 \right) \cdot \mathbf{n}_V \right\}_{t+\delta t} = 0, \tag{19}$$

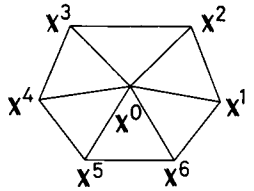

Figure 2. Subdomain of integration. Shown is an example of a subspace consisting of six elements, $\mathbf{x}^0$ being the location vector of the common nodal point and $\mathbf{x}^i$ ($i = 1, \ldots, 6$) being those of other nodal points

where $\mathbf{V}^*$ is a linearly interpolated velocity which is expressed as equation (14) in each triangular element; ε, though small, is a parameter which may be a function of the location of the common nodal points; $\mathbf{n}_V$ is a suitable unit vector in the x–y plane; $\mathbf{V}^k$ and $\mathbf{V}^0$ denote the velocities at the nodal point $\mathbf{x}^k$ and $\mathbf{x}^0$, respectively; summation on k is performed over the nodal points surrounding the point $\mathbf{x}^0$ (as shown in Figure 2); and the β_ks are constants such that

$$\sum_k \beta_k \mathbf{x}^k - \mathbf{x}^0 = \mathbf{0}, \qquad \sum_k \beta_k = 1, \tag{20}$$

although the combination of β_ks is not necessarily unique.

Treatment of boundary values

Internal flow. Discussions are limited to cases possessing solid boundaries and/or inlet and exit sections. At inlet and exit sections, mathematically it is necessary and sufficient to specify a velocity vector and a pressure gradient vector at any point as a function of time *a priori* in conformity with total mass balance, although it is rather difficult to concentrate the information outside to the inlet and exit sections virtually. On the other hand, at solid boundaries, only velocity vectors can be prescribed. Therefore it is necessary to introduce an expression for ∇p on the solid boundaries, which is formally obtained through equation (7), using the same finite element approximation as before by allocating a common nodal point on the boundary. In this procedure, however, relative errors having an order of the form (18) may be involved in estimating the first term of the left-hand side of equation (7), and since it is generally supposed that near the solid boundary

$$\left\| \left(\frac{\partial^2}{\partial x^2}, \frac{\partial^2}{\partial x\, \partial y}, \frac{\partial^2}{\partial y^2} \right) \mathbf{V} \right\| \gtrsim \frac{1}{h^2} \max_{\mathbf{x}^1, \mathbf{x}^2 \in S} |\mathbf{V}(\mathbf{x}^1) - \mathbf{V}(\mathbf{x}^2)|,$$

where S is the domain of integration, except near stagnation points, if any, the resultant formal expression will not give accurate information, and so this should be rejected. Alternatively, ∇p at the point (x_0, y_0) on the boundary can be obtained directly from equation (1) as

$$\nabla p_{(x_0, y_0)} = \left(-\frac{\partial}{\partial t}\mathbf{V} - (\mathbf{V}\cdot\nabla)\mathbf{V} + \frac{1}{Re}\Delta\mathbf{V} \right)_{(x_0, y_0)} \tag{21}$$

Thus ∇p at a nodal point on the boundary can be obtained by introducing the derivatives of $\mathbf{V}$ there in terms of velocity vectors at neighbouring nodal points by a finite difference method as follows. Let (x_i, y_i) $(i = 1, 2, 3, 4, 5)$ be co-ordinates of nodal points in a flow field near the point (x_0, y_0). Since $\mathbf{V}$ is assumed to be a vector field of class C^2, we obtain

$$\begin{aligned} \mathbf{V}(x_i, y_i) \cong\ & \mathbf{V}(x_0, y_0) + (x_i - x_0)\frac{\partial}{\partial x}\mathbf{V}(x_0, y_0) + (y_i - y_0)\frac{\partial}{\partial y}\mathbf{V}(x_0, y_0) \\ & + \tfrac{1}{2}(x_i - x_0)^2 \frac{\partial^2}{\partial x^2}\mathbf{V}(x_0, y_0) \\ & + (x_i - x_0)(y_i - y_0)\frac{\partial^2}{\partial x\, \partial y}\mathbf{V}(x_0, y_0) \\ & + \tfrac{1}{2}(y_i - y_0)^2 \frac{\partial^2}{\partial y^2}\mathbf{V}(x_0, y_0), \end{aligned} \tag{22}$$

from which the derivatives of $\mathbf{V}$ at (x_0, y_0) can be determined approximately in terms of $\mathbf{V}(x_0, y_0)$ and $\mathbf{V}(x_i, y_i)$ $(i = 1, 2, 3, 4, 5)$.

External flow. An infinitely extended, multiply-connected external flow region can be replaced for a numerical analysis by a multiply-connected region enclosed by an arbitrarily set-up section far from solid boundaries. The treatment of values at solid boundaries is the same as that in the previous section. Values of $\mathbf{V}$ and ∇p at the arbitrarily set-up section far from solid boundaries can be specified *a priori*, probably being asymptotic with at least one parameter such as a drag coefficient, for which other relation(s) leading to the parameter(s) should be supplemented.

System equations

System equations, which determine all of the velocity and pressure gradient vectors at every nodal point, consist of

(1) the discretized form of equation (13) using equations (14) and (15), constructed at every interior common nodal point (for the equation of motion)
(2) equation (19), constructed at every interior common nodal point (for the equation of continuity)
(3) the discretized form of equation (17) using equation (15), constructed at every interior common nodal point (for the compatibility condition)
(4) specified boundary values for $\mathbf{V}$ and ∇p (which may be supplemented with parameter(s))
(5) equations (21) and (22) for values of ∇p at nodal points on solid boundaries,

being supplemented with initial conditions if any.

Pressure field

Pressure itself at a specified time satisfies a total differential equation

$$\mathrm{d}p = \nabla p \cdot (\mathrm{d}x, \mathrm{d}y). \tag{23}$$

However, with the same accuracy as in equation (23), it would be proper to replace equation (23) by

$$\mathrm{d}p = \left\{ \beta^* \sum_k \beta_k \nabla p^k + (1 - \beta^*) \nabla p^0 \right\} \cdot (\mathrm{d}x, \mathrm{d}y), \tag{24}$$

where β^* is a parameter; β_k and superscripts k and 0 have the same meanings as in equations (19) and (20). Pressure itself can be obtained by integrating equation (24).

Weighting function

As for M_1, the following form is possible:

$$M_1 = \sum_m f_m(N_0^m) \tag{25}$$

where m, f_m, and N_0 denote an arbitrary real number (>0), any polynomial function such that $f_m(0) = 0$, and an area co-ordinate such that it assumes a value of unity when the point (x, y) coincides with the common nodal point, respectively. The simplest form of equation (25) is

$$M_1 = N_0^m \qquad (m > 0), \tag{26}$$

which will be used later. If the form (26) is used for M_2 and M_3, then the discretized forms of equations (16) and (17) become independent of m. Therefore it is suitable to define M_2 and M_3 as

$$M_2 = N_0, \tag{27}$$

$$M_3 = N_0. \tag{28}$$

In integration, use is made of the following formula:

$$\int N_1^\alpha N_2^\beta N_3^\gamma \, dS = 2A^* \frac{\Gamma(\alpha+1)\Gamma(\beta+1)\Gamma(\gamma+1)}{\Gamma(\alpha+\beta+\gamma+3)} \quad (\alpha > -1, \beta > -1, \gamma > -1), \tag{29}$$

where integration is performed over a triangular element; A^* denotes the area of the triangle; N_1, N_2 and N_3 are three mutually different area co-ordinates.

Solution procedure for the system equations

If the flow field is unsteady, the system equations can be solved directly step by step with respect to time with initial conditions since the system equations are linear in $\mathbf{V}(t+\delta t)$ and $\nabla p(t+\delta t)$, whereas, if the flow field is steady, the system equations constitute a system of simultaneous non-linear equations, which can be solved by means of a suitable method.

AN EXAMPLE OF THE ANALYSIS

Flow configuration

As an example the proposed finite element method using a pressure gradient method is applied to a two-dimensional, unsteady, recirculating, circular cavity flow in a horizontal plane: that is, Newtonian fluid enclosed in a circular cavity of radius unity is assumed to be initially at rest ($t < 0$) and at $t = 0$ the portion corresponding to a fixed half boundary of radius unity suddenly starts to move at a constant speed unity in its own curved plane in the counterclockwise direction.

Co-ordinate system

To describe the motion, a cylindrical polar co-ordinate (r, θ) with its origin at the centre of the cavity is used as well as a Cartesian co-ordinate system (x, y) in the usual orientation with the same origin, and without loss of generality the moving boundary is assumed to be $r = 1$, $-\pi < \theta < 0$.

Mesh generation

Regular meshes are generated as shown in Figure 3, equally spaced in the circumferential direction and alternately shifted in a half pitch among radial positions, so that the two singular points, $(x = 1, y = 0)$ and $(x = -1, y = 0)$, are not included among the nodal points. Besides, all the nodal points are located on concentric circles with equal spacing.

Initial conditions and boundary conditions

Initial conditions at $t = 0$ are expressed as

$$\begin{aligned} &\mathbf{V} = \mathbf{0}, && \text{for} \quad |r| < 1, \\ &\mathbf{V} = \mathbf{0}, && \text{for} \quad r = 1, 0 < \theta < \pi, \\ &\mathbf{V} = (-y, x), && \text{for} \quad r = 1, -\pi < \theta < 0. \end{aligned} \tag{30}$$

Boundary conditions are

$$\left.\begin{aligned} &\mathbf{V} = \mathbf{0}, && \text{for} \quad r = 1, 0 < \theta < \pi, \\ &\mathbf{V} = (-y, x), && \text{for} \quad r = 1, -\pi < \theta < 0. \end{aligned}\right\} \tag{31}$$

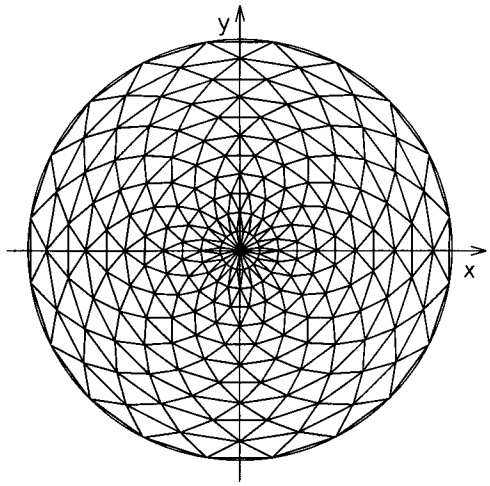

Figure 3. Meshes generated. Nodal points are assigned to all grid points

Special treatment at the centre of the cavity

Since the number of triangular elements commonly possessing the nodal points at the centre is much greater than that at other points, equation (19) and the discretized form of equation (17) at the centre would not give sufficiently good information, owing to their own forms, although they are necessary conditions within the precision of truncation errors. This does not apply to the case for the equation of motion, since not only a gradient of a weighting function but a weighting function itself are involved in equation (13). Therefore, at the centre, equation (19) and the discretized form of equation (17) can be replaced by the continuity of a pressure gradient, i.e.

$$(\nabla p)_{(0,0)} = \frac{1}{20}\sum(\nabla p), \tag{32}$$

where summation is performed over twenty nodal points surrounding the centre. In equation (32) truncation errors of order of h^2 are involved.

Numerical results

Figures 4 and 5 show patterns of streamlines and isobars for $Re = 100$, $t = 840/121$ ($m = 0{\cdot}5$, $6\varepsilon = 0{\cdot}01$, $\beta^* = 0{\cdot}5$, $\delta t = 20/121$, $h = 1/11$, $\mathbf{n}_V = (0, 1)$), where values of a stream function ψ are calculated directly by integrating the velocity component, for which in a three-dimensional vectorial notation

$$\mathbf{V} = \mathrm{curl}\,(0, 0, \psi), \tag{33}$$

and the pressure itself is due to equation (24). Figures 6 and 7 show patterns of streamlines and isobars for $Re = 100$, $t = \infty$ ($m = 0{\cdot}5$, $6\varepsilon = 0{\cdot}01$, $\beta^* = 0{\cdot}5$, $\delta t = 20/121$, $h = 1/11$, $\mathbf{n}_V = (0, 1)$), which correspond to the steady-state flow patterns (obtained at sufficiently large time).

DISCUSSION

Comparison with results by a finite element method and those by finite difference methods for a creeping flow

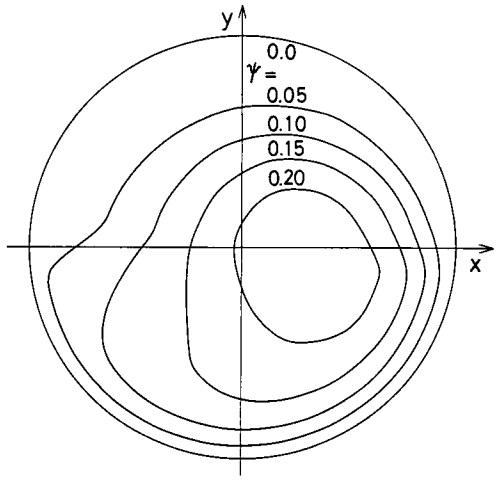

Figure 4. Streamlines in an unsteady flow in a circular cavity at $t = 840/121$ ($Re = 100$)

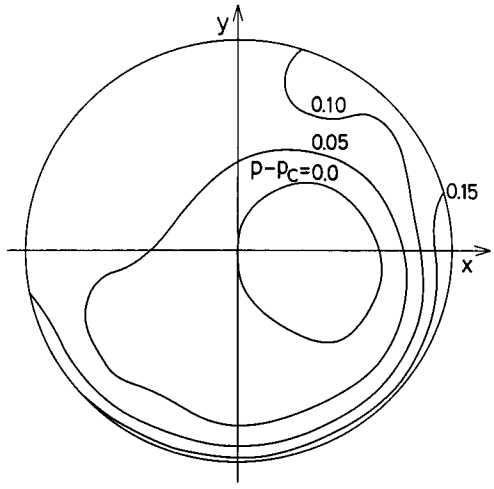

Figure 5. Isobars in an unsteady flow in a circular cavity at $t = 840/121$ ($Re = 100$)

For creeping flows, as an asymptotic analytical solution for $Re \to 0$, the stream function ψ and the pressure p can be expressed[7] as

$$\psi = -\tfrac{1}{4}(r^2-1) + \frac{r^2-1}{2\pi}\tan^{-1}\left(\frac{2r\sin\theta}{1-r^2}\right) + \sum_{k=1}^{\infty}\frac{1}{\beta_{0k}^2 J_0(\beta_{0k})}\{J_0(\beta_{0k}r) - J_0(\beta_{0k})\}\exp(-\beta_{0k}^2 t/Re) + \sum_{n=1,3,5,\ldots}\frac{4}{n\pi}\left[\sum_{k=1}^{\infty}\frac{1}{\beta_{nk}^2 J_n(\beta_{nk})}\{r^n J_n(\beta_{nk}) - J_n(\beta_{nk}r)\} \times \exp(-\beta_{nk}^2 t/Re)\right]\sin(n\theta), (t>0), \tag{34}$$

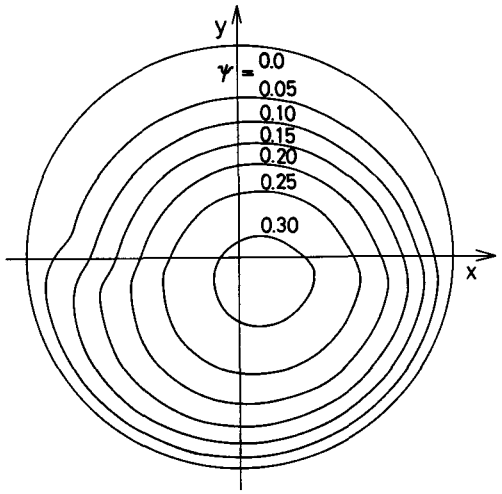

Figure 6. Streamlines at a sufficiently large time in a circular cavity, which correspond to those in a steady flow ($Re = 100$)

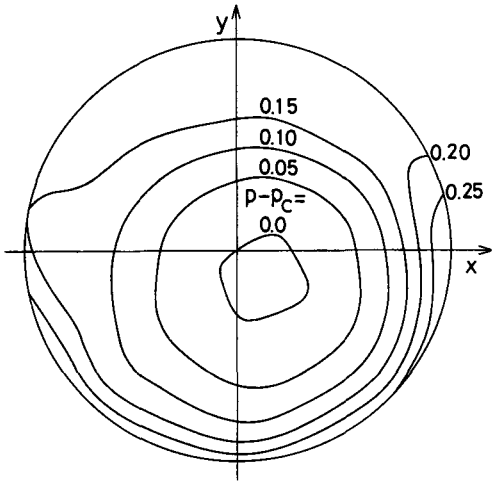

Figure 7. Isobars at a sufficiently large time in a circular cavity, which correspond to those in a steady flow ($Re = 100$)

$$p - p_c = \frac{1}{Re} \sum_{n=1,3,5,\ldots} \frac{4}{n\pi} \left\{ n + 1 + \sum_{k=1}^{\infty} \exp(-\beta_{nk}^2 t/Re) \right\} \times r^n \cos(n\theta), (t > 0), \tag{35}$$

where $\beta_{nk} (n = 0, 1, 3, 5, \ldots)$ is the kth positive zero of the Bessel function $J_{n+1}(x)$ and p_c is the pressure at the centre of the cavity. Using equations (34) and (35), numerical errors mainly due to discretization can be estimated, and the error behaviour with time can be compared among methods (a finite element method where $\mathbf{V}$ and ∇p are supposed to be dependent variables ($\mathbf{V}$–p method), and a finite difference modified pressure gradient method[7] where $\mathbf{V}$ and ∇p are supposed to be dependent variables); these are shown in Figures 8 and 9, where E_p and E_V denote measures of pressure errors and velocity errors, respectively, and are defined as

$$E_p = \frac{1}{n^*} \sum \{(p - p_c)_{\text{num.}} - (p - p_c)_{\text{anal.}}\}^2 / \{(p - p_c)_{\text{anal.}}\}^2, \tag{36}$$

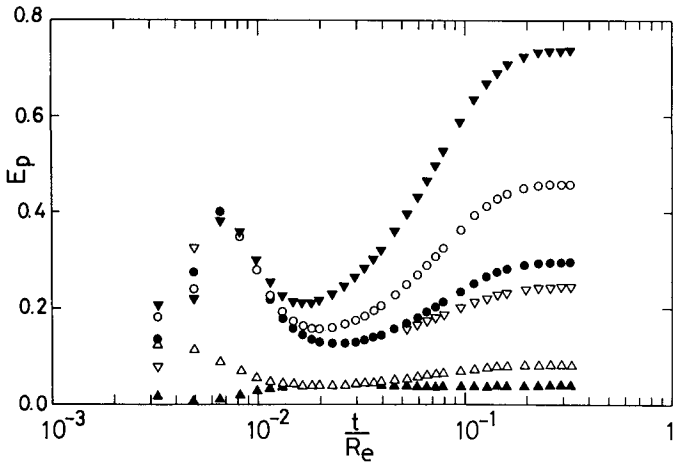

Figure 8. Error behaviour of E_p with time for different methods possessing the same parameters of common values ($Re = 0{\cdot}001, \delta t = 2 \times 10^{-4}/121$). $\nabla : m = 0{\cdot}25$ (the current FEM), $\bullet : m = 0{\cdot}5$ (the current FEM), $\circ : m = 0{\cdot}75$ (the current FEM), $\blacktriangledown : m = 1$ (the current FEM), $\blacktriangle$: a finite difference method using a modified pressure gradient methods, $\triangle$: a $\mathbf{V}$–p method. Values of parameters (ε, h, β^* and $\mathbf{n}_V$) used in the current FEM are the same as those corresponding to Figures 6 and 7

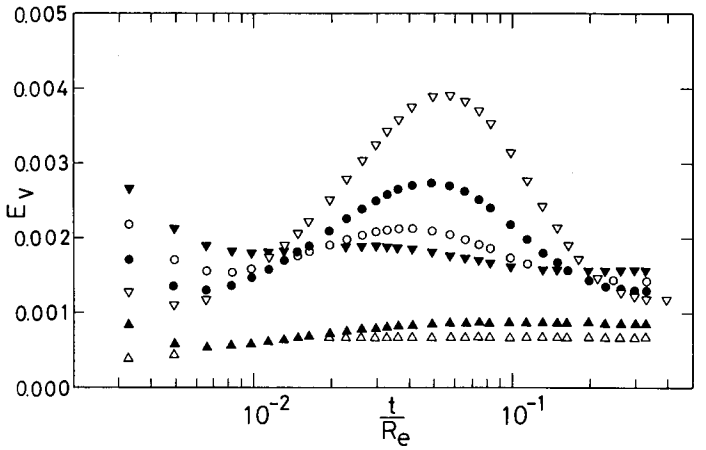

Figure 9. Error behaviour of E_V with time for different methods possessing the same parameters of common values ($Re = 0{\cdot}001, \delta t = 2 \times 10^{-4}/121$). $\nabla : m = 0{\cdot}25$ (the current FEM), $\bullet : m = 0{\cdot}5$ (the current FEM), $\circ : m = 0{\cdot}75$ (the current FEM), $\blacktriangledown : m = 1$ (the current FEM), $\blacktriangle$: a finite difference method using a modified pressure gradient method, $\triangle$: a $\mathbf{V}$–p method. Values of parameters (ε, h, β^* and $\mathbf{n}_V$) used in the current FEM are the same as those corresponding to Figures 6 and 7

$$E_V = \frac{1}{n^*} \sum |\mathbf{V}_{\text{num.}} - \mathbf{V}_{\text{anal.}}|^2, \tag{37}$$

where n^* is the total number of points to be evaluated, and the subscripts num. and anal. mean 'obtained numerically' and 'obtained analytically', respectively. In Figures 8 and 9, all the discretizing methods possess the same spatial division in a radial direction and the same time increment, and for the estimation of equations (36) and (37), pressure and velocity are evaluated at points over two concentric circles ($r = 10/11$, $6/11$) ($n^* = 40$). As far as the current spatial division and time increment at a specified small value of Re are concerned, as in Figures 8 and 9, the current finite element method produces errors a little greater than those of the finite

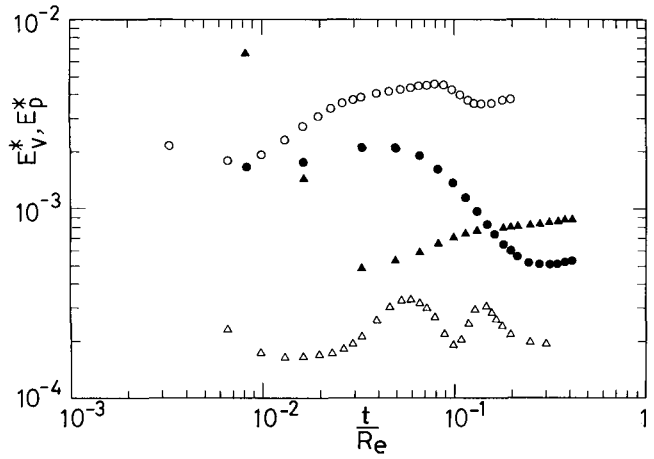

Figure 10. Comparison between results by a finite element method and a finite difference method using a pressure gradient method. ●: E_V^* for $Re = 10$, ○: E_V^* for $Re = 100$, ▲: E_p^* for $Re = 10$, △: E_p^* for $Re = 100$. Values of parameters (ε, h, β^* and n_V) used in the finite element method are the same as those corresponding to Figures 6 and 7. Values of δt are 10/121 for $Re = 10$ and 20/121 for $Re = 100$

difference methods, though among the results by the finite element method the one using a power of $m = 0{\cdot}5$ (or 0·25) is found to give relatively good results.

Comparison with results at a moderate Reynolds number

For a moderate Reynolds number flow in this configuration, no analytical solutions have been found, so that comparison is made between results by a finite difference method using a pressure gradient method and those by the current finite element method; these are shown in Figure 10, where E_p^* and E_V^* denote measures of pressure and velocity differences between the results, respectively, and are defined as

$$E_p^* = \frac{1}{n^*}\sum\{(p - p_c)_E - (p - p_c)_D\}^2, \tag{38}$$

$$E_V^* = \frac{1}{n^*}\sum|(\mathbf{V})_E - (\mathbf{V})_D|^2, \tag{39}$$

where the subscripts E and D denote 'obtained by the current finite element method' and 'obtained by finite difference method using the modified pressure gradient method',[7] respectively. In Figure 10, the situation for discretization in space is the same as in a creeping flow, and for the estimation of equations (38) and (39), pressure and velocity are evaluated at points over two concentric circles ($r = 9/11$, $5/11$) ($n^* = 40$). As far as pressure gradient methods are concerned, as shown in Figure 10 no remarkable differences between finite element methods and finite difference methods can be found.

Effects of a parameter introduced in equation (19)

Unless the absolute value of the parameter ε in equation (19) is zero or too small, flow fields obtained using two different values of ε are in quite good agreement with each other in the sense that the change of ε by a factor of two produces variations in p and $\mathbf{V}$ (defined similarly as in equations (38) and (39)) of the order of $10^{-7} \sim 10^{-8}$ at a Reynolds number of 10.

CONCLUSION

A pressure gradient method is applied to a finite-element-method flow analysis for a two-dimensional incompressible Newtonian fluid flow. Using triangular elements and by linearly interpolating the unknown vector fields, discretized system equations can be derived with suitable weighting functions possessing a parameter independent of other dimensionless parameters such as a Reynolds number. An example of numerical analysis of the system equations is presented for an unsteady-state development of a recirculating circular cavity flow, and the flow features obtained are found to be in good agreement with those obtained by other methods.

NOTATION

$\mathbf{dc}$	line-element vector along the contour of the domain of integration
dc	$\equiv \lvert\mathbf{dc}\rvert$
$\mathbf{dS}$	area-element vector normal to the surface
dS	$\equiv \lvert\mathbf{dS}\rvert$
E_p	defined in equation (36)
E_p^*	defined in equation (38)
E_V	defined in equation (37)
E_V^*	defined in equation (39)
h	characteristic length of a triangular element
m	parameter introduced in equation (26)
M_1, M_2, M_3	weighting functions
$\mathbf{n}$	outward unit normal (parallel to the flow plane) at the contour of the domain of integration
N_0, N_1, N_2, N_3	area co-ordinates
$\mathbf{n}_V$	unit vector introduced in equation (19)
p	pressure
r	radial co-ordinate in a cylindrical polar co-ordinate system
Re	Reynolds number
t	time
$\mathbf{V}$	velocity vector
x	co-ordinate in a Cartesian co-ordinate system (parallel to the flow plane)
y	co-ordinate in a Cartesian co-ordinate system (parallel to the flow plane)
β^*	parameter introduced in equation (24)
β_k	constant introduced in equation (20)
δt	time increment
ε	parameter introduced in equation (19)
θ	tangential co-ordinate in a cylindrical polar co-ordinate system
ψ	stream function
∇	gradient operator
Δ	Laplacian operator

REFERENCES

1. R. H. Gallagher, J. T. Oden, O. C. Zienkiewicz, T. Kawai and M. Kawahara (eds), *Finite Elements in Fluids*, Volume 5, Wiley, 1984.
2. R. H. Gallagher, D. H. Norrie, J. T. Oden and O. C. Zienkiewicz (eds), *Finite Elements in Fluids*, Volume 4, Wiley, 1982.

3. D. A. Anderson, J. C. Tannehill and R. H. Pletcher, *Computational Fluid Mechanics and Heat Transfer*, McGraw-Hill, 1984.
4. M. J. Crochet, A. R. Davies and K. Walters, *Numerical Simulation of Non-Newtonian Flow*, Elsevier, 1984.
5. T. M. Shih, *Numerical Heat Transfer*, Hemisphere, 1984.
6. O. C. Zienkiewicz, J. P. S. R. Gago and D. W. Kelley, 'The hierarchical concept in finite element analysis', *Computers and Structures*, **16**, 53–65 (1983).
7. Y. Mochimaru, 'Improvement of a pressue gradient method and its application to an unsteady flow problem', *Int. j. numer. methods fluids*, **5**, 627–635 (1985).
8. J. E. Akin, *Application and Implementation of Finite Element Methods*, Academic Press, 1982.
9. O. C. Zienkiewicz, *The Finite Element Method*, McGraw-Hill, 1977.